

Copyright © 1992, by the author(s).
All rights reserved.

Permission to make digital or hard copies of all or part of this work for personal or classroom use is granted without fee provided that copies are not made or distributed for profit or commercial advantage and that copies bear this notice and the full citation on the first page. To copy otherwise, to republish, to post on servers or to redistribute to lists, requires prior specific permission.

**DRY TURBULENCE FROM A TIME-DELAYED
CHUA'S CIRCUIT**

by

A. N. Sharkovsky, Yu. Maistrenko, Ph. Deregel,
and L. O. Chua

Memorandum No. UCB/ERL M92/76

21 July 1992

UCB/ERL M92/76

**DRY TURBULENCE FROM A TIME-DELAYED
CHUA'S CIRCUIT**

by

A. N. Sharkovsky, Yu. Maistrenko, Ph. Deregel,
and L. O. Chua

Memorandum No. UCB/ERL M92/76

21 July 1992

ELECTRONICS RESEARCH LABORATORY

College of Engineering
University of California, Berkeley
94720

TITLE PAGE

**DRY TURBULENCE FROM A TIME-DELAYED
CHUA'S CIRCUIT**

by

A. N. Sharkovsky, Yu. Maistrenko, Ph. Deregel,
and L. O. Chua

Memorandum No. UCB/ERL M92/76

21 July 1992

ELECTRONICS RESEARCH LABORATORY

College of Engineering
University of California, Berkeley
94720

DRY TURBULENCE FROM A TIME-DELAYED CHUA'S CIRCUIT

A.N. SHARKOVSKY, Yu. MAISTRENKO

Institute of Mathematics of the Ukrainian Academy of Sciences
Kiev, Ukraine

Ph. DEREGEL, L. O. CHUA

Department of Electrical Engineering and Computer Sciences,
University of California,
Berkeley, CA 94720, USA

July 21, 1992

Abstract

In this paper, we consider an infinite-dimensional extension of Chua's circuit (Fig.1) obtained by replacing the left portion of the circuit composed of the capacitance C_2 and the inductance L by a lossless transmission line as shown in Fig.2. As we shall see, if the remaining capacitance C_1 is equal to zero, the dynamics of this so-called time-delayed Chua's circuit can be reduced to that of a scalar nonlinear difference equation. After deriving the corresponding 1-D map, it will be possible to determine without any approximation the analytical equation of the stability boundaries of cycles of *every* period n . Since the stability region is non-empty for each n , this proves rigorously that the time-delayed Chua's circuit exhibits the "*period-adding*" phenomenon where every two consecutive cycles are separated by a chaotic region.

This work has been supported in part by the Office of Naval research under grant N0014-89-J-1402 and the National Science Foundation under grant MIP-8912639

1 Introduction

Our starting point is the Chua's circuit shown in figure 1. Let us first add a dc bias voltage source in series with the Chua diode ¹. Next, let us replace the left part of Chua's circuit, composed of a capacitance and an inductance in parallel, by a lossless transmission line where a short circuit is connected across the left terminal pair. Since the transmission line introduces a *time delay* to the signal originating from the right, the resulting Chua's transmission line circuit, shown in Fig.2, will henceforth be referred to the *time-delayed Chua's circuit*.

To study this new dynamical system, we shall use the approach of "dry" turbulence developed by Alexander Sharkovsky ². Indeed, the system exhibits characteristics similar to those present in turbulence, such as intermittency, formation of coherent structures, and the emergence of vortices of decreasing sizes via a cascade process. The term "dry" refers to a system where there is no viscosity, where arbitrarily high harmonics are present. Since all of these phenomena are infinite-dimensional in nature, it follows that in order to carry out a realistic study of the time-delayed Chua's circuit, we cannot make any finite-dimensional approximations.

This is a difficult mathematical problem. It is thus remarkable that our system can be reduced to a difference or differential-difference equation. In the first case ($C_1 = 0$), we obtain a nonlinear scalar difference equation. After deriving the corresponding map and its invariant interval, it will be possible to study the dynamics of the system. In particular, under certain conditions, we shall be able to find the analytical equation in the parameter space of the windows of stability corresponding to limit cycles of any period.

The second case ($C_1 \neq 0$) leads to a nonlinear differential-difference equation. Very few mathematical tools are currently available for studying such systems. Fortunately, for small values of C_1 , computer simulations show that the *qualitative* behaviors are in most cases similar to the behaviors reported in this paper, when $C_1 = 0$.

2 The circuit and its equations

2.1 The time-delayed Chua's circuit

The time-delayed Chua's circuit is shown in Fig.2, where the $v - i$ characteristic of Chua's diode N_R is shown in Fig.3. The capacitance C_2 and the inductance L from the original Chua's circuit, have been replaced by a transmission line. From a physical point of view, this is a logical extension to the infinite-dimensional case obtained by adding infinitely many

inductors in series and capacitors in parallel. The resulting series inductance and the parallel capacitance per unit length of the line are denoted by L and C , respectively. The characteristic impedance of the line is denoted by $Z = (\frac{L}{C})^{\frac{1}{2}}$.

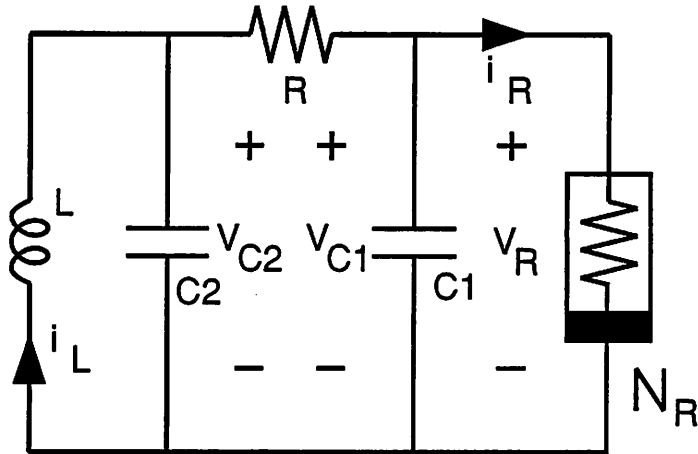


Figure 1: Chua's circuit

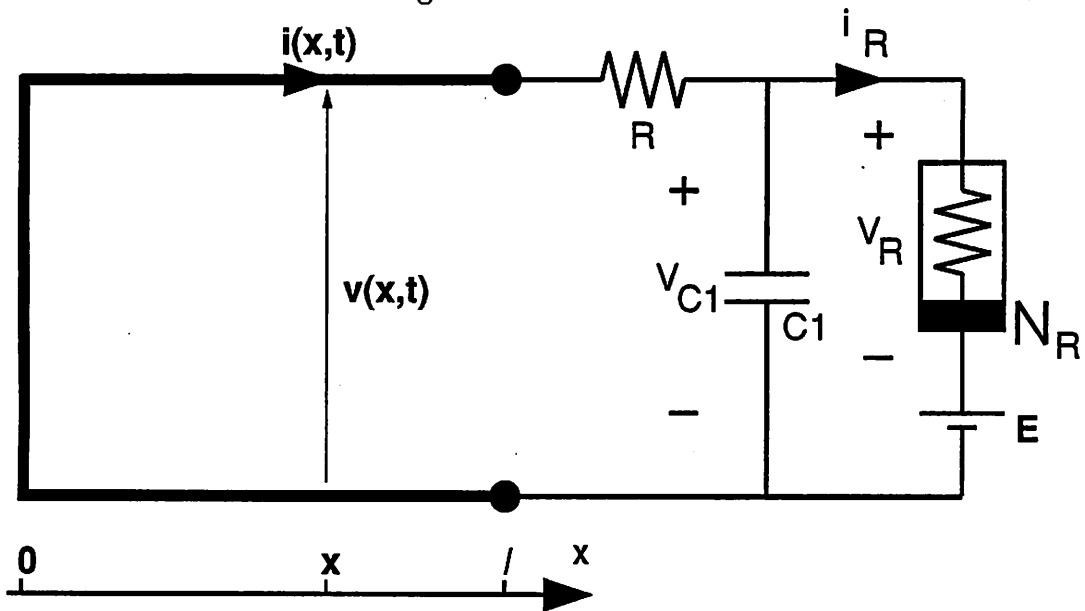


Figure 2: Time-delayed Chua's circuit

The right part C_{right} of the time delayed Chua's circuit can be interpreted as a generator of chaotic signals. The resulting waves will propagate, without loss along the transmission line. The wave is reflected at the end of the line ($x = 0$) with a phase shift of π and returns

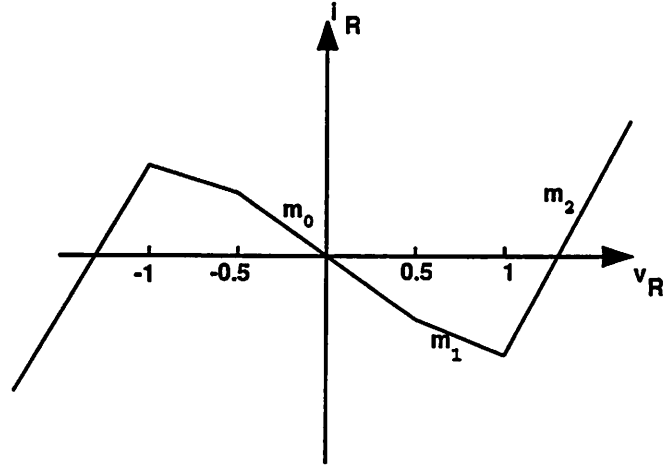


Figure 3: v - i characteristic $i_R = G(v_R)$ of Chua's diode

towards $x = l$. This phenomenon occurs as long as there is an impedance mismatch between the characteristic impedance Z of the transmission line and the small-signal impedance of the right part of the circuit C_{right} . One may notice that an impedance match makes sense only for small signals, when N_R is linear.

At dc, the time-delayed Chua's circuit is equivalent to the circuit shown in fig.4. From now on, we shall assume that the two slopes m_1 and m_2 are equal. The characteristics of the Chua's diode and the load line are given in the v_R - i_R plane in fig.4. The dc bias voltage breaks the symmetry of the system. In the case $m_0 < 0$ and $m_2 > 0$, there may be one or three operating points, depending on the value of the resistance R in the circuit. If $m_0 = m_1$ and m_2 were positive, the system would remain stable and is therefore not particularly interesting. If they were both negative, the system may become unbounded. In this paper, we have $m_0 = m_1 < 0$ and $m_2 > 0$.

2.2 Equations for the lossless transmission line

Assuming that there are no losses in the transmission line, the relation between the voltage $v(x, t)$ and the current $i(x, t)$ at time t and at a distance x from the left origin is given by :

$$\begin{cases} \frac{\partial v(x, t)}{\partial x} = -L \frac{\partial i(x, t)}{\partial t} \\ \frac{\partial i(x, t)}{\partial x} = -C \frac{\partial v(x, t)}{\partial t} \end{cases} \quad (1)$$

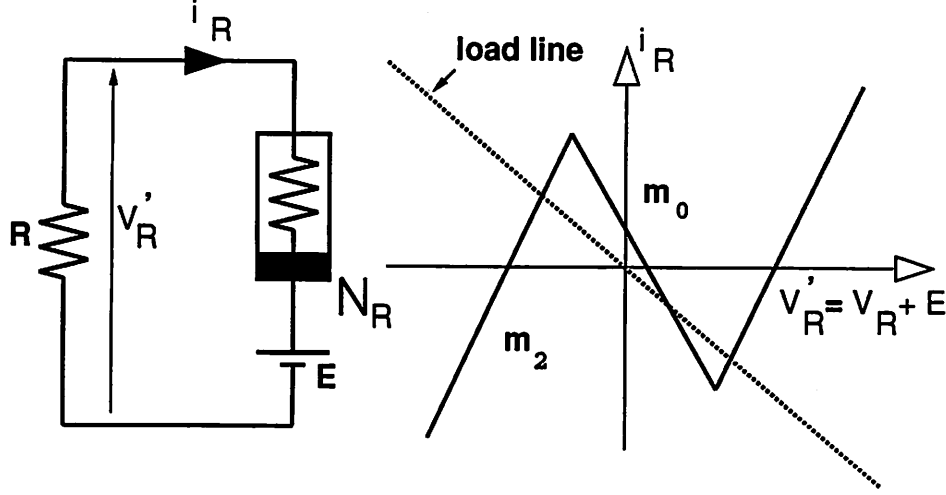


Figure 4: Simplified time-delayed Chua's circuit at equilibrium

where L and C denote the inductance and capacitance per unit length of the transmission line. By eliminating i or v , from these two equations, we obtain :

$$\frac{\partial^2 v(x,t)}{\partial x^2} = LC \frac{\partial^2 v(x,t)}{\partial t^2} \quad (2)$$

The general solution of equation (2) is of the form:

$$v(x,t) = a \left(t - \frac{x}{\nu} \right) + b \left(t + \frac{x}{\nu} \right) \quad (3)$$

where the two *scattering variables* a and b represent the incident and the reflected waves, respectively, at the velocity $\nu = (LC)^{-\frac{1}{2}}$.

From (2) and (3) it immediately follows that

$$i(x,t) = \frac{1}{Z} \left[a \left(t - \frac{x}{\nu} \right) - b \left(t + \frac{x}{\nu} \right) \right] \quad (4)$$

where $Z = \left(\frac{L}{C} \right)^{\frac{1}{2}}$ is the characteristic impedance of the transmission line.

2.3 Boundary conditions

There are two boundary conditions, one at each end of the transmission line. First, the line is shorted at $x = 0$. Second, at $x = l$, the line is connected to the right portion of the Chua's circuit, denoted by C_{right} . These two boundary conditions can be expressed in the form:

$$\begin{cases} v(0, t) = 0 \\ i(l, t) = F\left(v(l, t), i(l, t), \frac{\partial v(l, t)}{\partial t}, \frac{\partial i(l, t)}{\partial t}\right) \end{cases} \quad (5)$$

The first boundary condition implies that

$$a\left(t - \frac{x}{\nu}\right) = -b\left(t - \frac{x}{\nu}\right) \equiv \Phi\left(t - \frac{x}{\nu}\right) \quad (6)$$

where we have introduced the new symbol Φ , in place of the incident wave $a(\cdot)$ since both incident and reflected waves are derived from the same function.

Hence, in term of the incident wave $\Phi(x, t)$, the solution of (1) is of the form :

$$\begin{cases} v(x, t) = \Phi\left(t - \frac{x}{\nu}\right) - \Phi\left(t + \frac{x}{\nu}\right) \\ i(x, t) = \frac{1}{Z} \left[\Phi\left(t - \frac{x}{\nu}\right) + \Phi\left(t + \frac{x}{\nu}\right) \right] \end{cases} \quad (7)$$

The second boundary condition is determined by the terminating nonlinear subcircuit C_{right} . By expressing the current $i(x, l)$ as the sum of the current in the Chua's diode and that in the capacitor C_1 , we obtain :

$$\begin{aligned} i(l, t) &= F\left(v(l, t), i(l, t), \frac{\partial v(l, t)}{\partial t}, \frac{\partial i(l, t)}{\partial t}\right) \\ &= G\left(v(l, t) - E - Ri(l, t)\right) + C_1 \frac{\partial(v(l, t) - Ri(l, t))}{\partial t} \end{aligned} \quad (8)$$

Where $G(\cdot)$ is the $v - i$ characteristic of the Chua's diode. Given the initial conditions at $t=0$, i.e. the value of $v(x, 0), i(x, 0), \frac{\partial v(x, 0)}{\partial t}$ and $\frac{\partial i(x, 0)}{\partial t}$ for $x \in [0, l]$, equations (1) and (5) completely determine the behavior of the system.

2.4 Form of the solutions

Considering equation (1) and the boundary condition (5) at $x = 0$, we have shown that $i(x, t)$ and $v(x, t)$ can be expressed as a function of one of the scattering variables, namely the incident wave $a = \Phi$. The problem consists of determining this function Φ from the initial condition, i.e. the function Φ on $[-\frac{l}{\nu}, \frac{l}{\nu}]$. Physically, this initial condition corresponds to the current and the voltage in the transmission line at $t = 0$, since $v(x, 0)$ and $i(x, 0)$ are uniquely defined for $0 \leq x \leq l$ upon substituing $\Phi(-\frac{x}{\nu})$ and $\Phi(\frac{x}{\nu})$ into (7) at $t = 0$. As we shall see, the evolution of Φ will depend crucially on the boundary conditions at $x=l$.

3 Analysis of the system without the capacitance C_1

3.1 Introduction

In this section, we shall consider the idealized time-delayed Chua's circuit without the capacitance C_1 . As explained above the problem consists of determining the scattering variable Φ . In the case $C_1 = 0$, the function F which represents the boundary condition at $x = l$ becomes:

$$F(v(l, t), i(l, t)) = G(v(l, t) - Ri(l, t) - E) \quad (9)$$

where G is the equation of the characteristic of the Chua's diode. As we shall see, from this equation it will be possible to derive a map M such that ³ :

$$\Phi\left(t + \frac{l}{\nu}\right) = M\left(\Phi\left(t - \frac{l}{\nu}\right)\right) \quad (10)$$

In order to study this difference equation, the dynamics of the map M will be first examined. As we shall see this very simple 1-D map exhibits rather complicated dynamics from which it will be easy to determine that of Φ .

3.2 Construction of the map M

In order to derive the map M , let us first examine the boundary condition at $x = l$:

$$i(l, t) = G(v(l, t) - Ri(l, t) - E) \quad (11)$$

Substituting (7) into (11), we obtain :

$$\frac{1}{Z} \left[\Phi\left(t - \frac{T}{2}\right) + \Phi\left(t + \frac{T}{2}\right) \right] = G\left(\Phi\left(t - \frac{T}{2}\right) - \Phi\left(t + \frac{T}{2}\right) - \frac{R}{Z} \left(\Phi\left(t - \frac{T}{2}\right) + \Phi\left(t + \frac{T}{2}\right)\right) - E\right) \quad (12)$$

where $\frac{T}{2} \equiv \frac{l}{\nu}$. By introducing the function $\phi(t) \equiv \Phi\left(t - \frac{T}{2}\right)$, (12) becomes :

$$\phi(t) + \phi(t + T) = ZG\left(\left(1 - \frac{R}{Z}\right)\phi(t) - \left(1 + \frac{R}{Z}\right)\phi(t + T) - E\right) \quad (13)$$

If we define :

$$\begin{cases} \xi &= \frac{1}{\sqrt{2}} [v(l, t) - Ri(t, t)] &= \frac{1}{\sqrt{2}} \left(\left(1 - \frac{R}{Z}\right)\phi(t) - \left(1 + \frac{R}{Z}\right)\phi(t + T) \right) \\ \eta &= \frac{Z}{\sqrt{2}} i(l, t) &= \frac{1}{\sqrt{2}} (\phi(t) + \phi(t + T)) \end{cases} \quad (14)$$

Then equation (13) can be recast into the form :

$$\eta = \frac{Z}{\sqrt{2}} G(\sqrt{2}\xi - E) \quad (15)$$

Inverting the system (14), we obtain:

$$\begin{cases} \phi(t) &= \frac{1}{\sqrt{2}} \left[\xi + \left(1 + \frac{R}{Z}\right) \eta \right] \\ \phi(t+T) &= \frac{1}{\sqrt{2}} \left[-\xi + \left(1 - \frac{R}{Z}\right) \eta \right] \end{cases} \quad (16)$$

where η and ξ are linked by the equation (15). In order to simplify the notation, let us introduce the function g :

$$g(\xi) = \frac{Z}{\sqrt{2}} G(\sqrt{2}\xi) \quad (17)$$

Our aim is now to find a direct relation between $\phi(t)$ and $\phi(t+T)$. Let us denote by B the basis (ξ, η) . In the basis $B_0(\xi', \eta')$ where $\xi' = \xi - \frac{E}{\sqrt{2}}$ and $\eta' = \eta$ (see Fig 5) :

$$\eta' = g(\xi') \quad (18)$$

Let us consider first the case $R=0$. In this case (16) becomes :

$$\begin{cases} \phi(t) &= \frac{1}{\sqrt{2}}(\xi + \eta) = X \\ \phi(t+T) &= \frac{1}{\sqrt{2}}(-\xi + \eta) = Y \end{cases} \quad (19)$$

This corresponds to a rotation through an angle $\frac{\pi}{4}$. Therefore let us consider the new basis $B_1(X, Y)$, which is the basis B_0 rotated by $\frac{\pi}{4}$ as shown in Fig.5. In this basis B_1 , if $R = 0$, the abscissa and the ordinate correspond to $\phi(t)$ and $\phi(t+T)$, respectively.

In the basis $B_1(X, Y)$, it is now easier to examine the case $R \neq 0$. We look for a basis $B_2(x, y)$ where $\phi(t+T)$ and $\phi(t)$ will fall directly on the new set of $x - y$ axis. Therefore, the equation of the new x -axis of B_2 in B_1 is $\phi(t+T) = 0$ and that of the y -axis is $\phi(t) = 0$. Thus :

$$\begin{cases} x = 0 &\leftrightarrow X = \frac{R}{R+2Z} Y \\ y = 0 &\leftrightarrow Y = -\frac{Z}{R+2Z} X \\ x = y &\leftrightarrow Y = \left(1 + \frac{Z}{R}\right) X \end{cases} \quad (20)$$

The transformation from the basis B_1 to B_2 is a rotation matrix :

$$\frac{1}{\sqrt{1 + \frac{R^2}{(R+2Z)^2}}} \begin{pmatrix} 1 & -\frac{R}{R+2Z} \\ \frac{R}{R+2Z} & 1 \end{pmatrix} \quad (21)$$

As shown in Fig.5, in B_2 , it is possible to calculate $\phi(t+nT)$ from $\phi(t)$:

$$\begin{cases} X_1 &= \phi(t) \\ X_2 &= \phi(t+T) \\ X_3 &= \phi(t+2T) \\ \vdots & \\ X_{n+1} &= \phi(t+nT) \\ \vdots & \end{cases} \quad (22)$$

We now have to find the equation of Chua's diode in the basis B_2 . It will allow us to

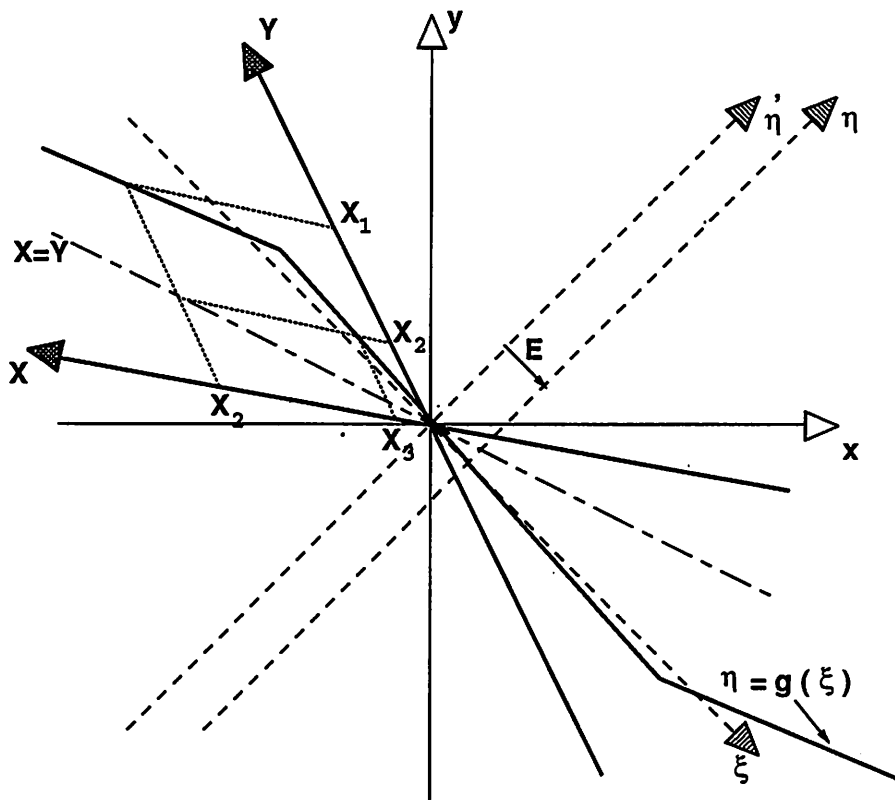


Figure 5: Characteristic of Chua's diode in the bases B, B_0, B_1 and B_2

study the map M directly. The fact that the equation of this diode is piecewise-linear will considerably simplify our work. The three-segment function is determined by the four points P_1, P_2, P_3 and P_4 (see Fig.6). P_2 and P_3 are the two break points. P_1 and P_4 provide a second point to determine the outer segments at $V_R = -2$ and $V_R = 2$, respectively..

The coordinates of these points will be given successively in the basis B_0, B_1 and B_2 .

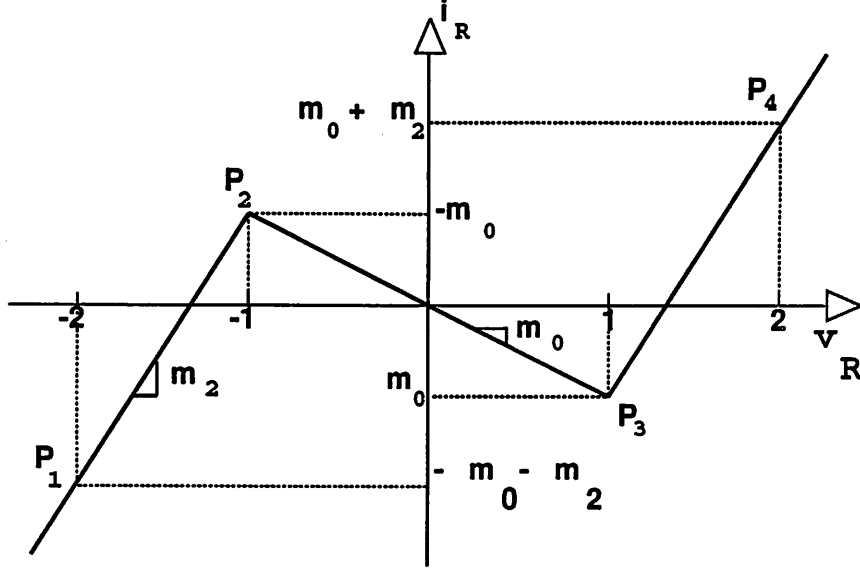


Figure 6: Determination of the characteristic of Chua's diode by the four points P_1, P_2, P_3 and P_4

In $B_0(\xi, \eta')$:

$$\begin{cases} P_1 = (-2 + E', -m_0 - m_2) \\ P_2 = (-1 + E', -m_0) \\ P_3 = (1 + E', m_0) \\ P_4 = (2 + E', m_0 + m_2) \end{cases} \quad (23)$$

where $E' = \frac{E}{\sqrt{2}}$

In $B_1(X, Y)$:

$$\begin{cases} P_1 = (-2 + E' - m_0 - m_2, 2 - E' - m_0 - m_2) = (x'_1, y'_1) \\ P_2 = (-1 + E' - m_0, 1 - E' - m_0) = (x'_2, y'_2) \\ P_3 = (1 + E' + m_0, -1 - E' + m_0) = (x'_3, y'_3) \\ P_4 = (2 + E' + m_0 + m_2, -2 - E' + m_0 + m_2) = (x'_4, y'_4) \end{cases} \quad (24)$$

In $B_2(x, y)$

$$P_{i \in \{1..4\}} = \frac{1}{\sqrt{1 + \frac{R^2}{(R+2Z)^2}}} \left(\frac{R}{R+2Z} x'_i + y'_i, -x'_i + \frac{R}{R+2Z} y'_i \right) = (x''_i, y''_i) \quad (25)$$

The four points P_1, P_2, P_3 and P_4 determine the equation of the Chua's diode characteristic in the basis B_2 . As it is shown in fig.7, the resulting map M may be multivalued. In

order to determine ϕ via (10), M has to be single-valued. Therefore we have to determine the condition on the parameters of the system that lead to this case. Provided that P_1 and P_4 remains symmetric with respect to the middle of the segment $[P_2, P_3]$, there are four possible cases, as shown in Figure 7:

$$\begin{cases} a) x_1'' < x_2'' < x_3'' < x_4'' \\ b) x_1'' < x_3'' < x_2'' < x_4'' \\ c) x_4'' < x_2'' < x_3'' < x_1'' \\ d) x_4'' < x_3'' < x_2'' < x_1'' \end{cases} \quad (26)$$

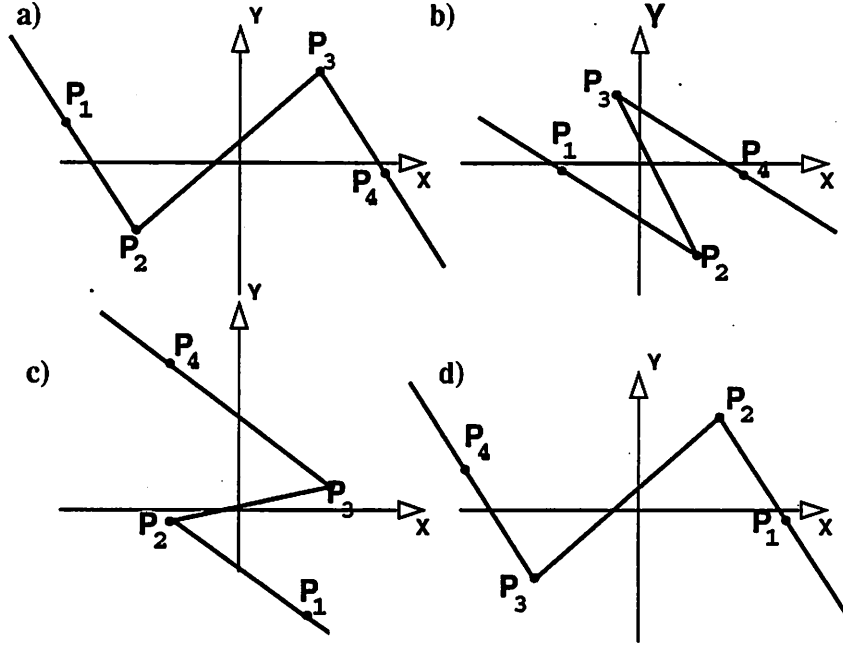


Figure 7: Single-valued and multivalued map M

In the cases a and d , the map is single-valued and it is possible to write its equation explicitly as follows.

$$\begin{cases} g(X) = nm_2 X + \frac{1}{2}(nm_0 - nm_2)(|X - x_3''| - |X - x_2''|) & \text{in case } a \\ g(X) = nm_2 X + \frac{1}{2}(nm_0 - nm_2)(|X - x_2''| - |X - x_3''|) & \text{in case } d \end{cases} \quad (27)$$

where nm_0 and nm_2 are the slopes of the characteristic of Chua's diode in the basis B_2 :

$$\begin{cases} nm_0 = \frac{(y_3'' - y_2'')}{(x_3'' - x_2'')} = \frac{-Z + (Z - R)m_0}{Z + (Z + R)m_0} \\ nm_2 = \frac{(y_4'' - y_3'')}{(x_4'' - x_3'')} = \frac{-Z + (Z - R)m_2}{Z + (Z + R)m_2} \end{cases} \quad (28)$$

3.3 Dynamics of the map M

In the previous section, we have found an explicit equation of the map M leading to a difference equation which determines the function ϕ . We now examine the dynamics of the 1-D map M. In other words, given X_1 , what will $\Phi(X_1 + nT) = M^n(X_1)$ be? To study this map, we first need to determine its invariant interval I.

3.3.1 Determination of the invariant interval I

As we did in deriving the equation for M, let us first consider the case $R=0$. If $E' = 0$, the map M is symmetric as shown in Fig.8. In this case the invariant interval I is :

$$I = \left[-\frac{1-m_0}{2}, \frac{1-m_0}{2} \right] \quad (29)$$

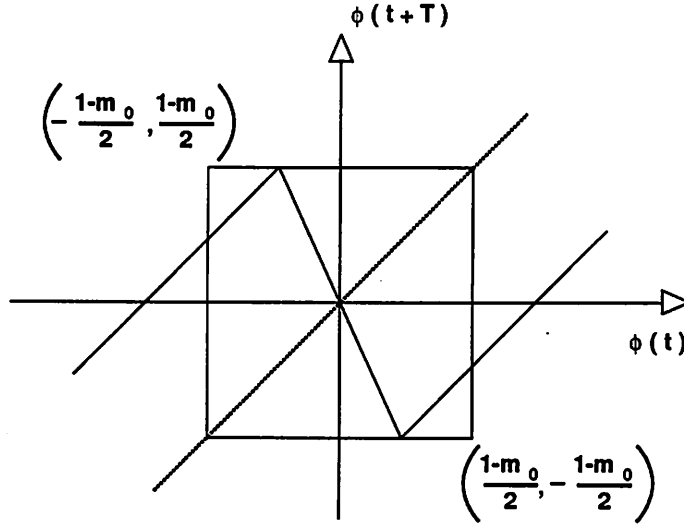


Figure 8: Map in the case $R=0$ and $E=0$

When $E' = 0$ the system is symmetric with respect to the origin, let us denote by M_0 the corresponding map. For the same parameters m_0, m_2 and R , if we introduce a dc bias voltage, the characteristics of Chua's diode will be translated along the short vector $(e_x E', e_y E')$, parallel to the axis ξ , and indicated by E in Fig.5. Let us denote by $M_{E'}$ the corresponding map and by x a point:

$$\begin{cases} M_{E'}(x) = M_0(x - e_x E') + e_y E' \\ M_{-E'}(-x) = M_0(-x + e_x E') - e_y E' = -M_{E'}(x) \end{cases} \quad (30)$$

It is clear that if we use an opposite dc bias voltage, the behavior of the system is identical up to symmetry with respect to the y axis. Therefore we can limit our study to $E' > 0$. In this case, the presence of the dc bias voltage E' is equivalent to a translation of the characteristic of Chua's diode to the right. Depending on the value of E' , two cases must be considered as shown in Fig.9.

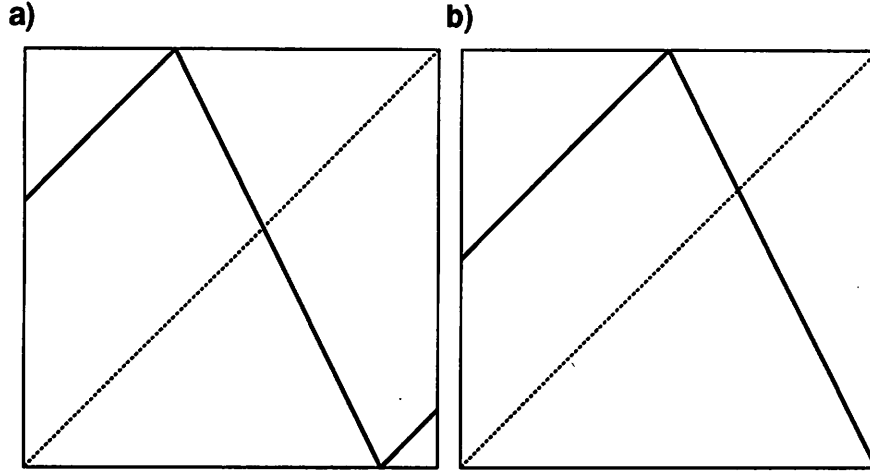


Figure 9: Three-segment and two-segment map M in the case $R=0$ and $E \neq 0$

$$\begin{cases} \text{a)} & E' < -m_0 & \text{then} & I = \left[\frac{-1+m_0+E'}{2}, \frac{1-m_0+E'}{2} \right] \\ \text{b)} & -m_0 < E' < 1 & \text{then} & I = \left[\frac{1-m_0}{2} + \frac{(-1+3m_0)E'}{2(1+m_0)}, \frac{1-m_0+E'}{2} \right] \end{cases} \quad (31)$$

In the case $R \neq 0$, we obtain :

if $0 < |E'| < Z|m_0|$,

$$I = \left[\frac{-1 + E' + (Z - R)m_0}{2}, \frac{1 + E' - (Z + R)m_0}{2} \right] \quad (32)$$

if $Z|m_0| < |E'| < 1+R|m_0|$,

$$I = \left[\frac{-1 + E' + (Z - R)m_0}{2} - \frac{(1 + E' + Rm_0)(1 - (Z - R)m_0)}{1 + (Z + R)m_0}, \frac{1 + E' - (Z - R)m_0}{2} - \frac{(1 + E' + Rm_0)(1 - (Z - R)m_0)}{1 + (Z + R)m_0} \right] \quad (33)$$

Let the invariant interval of the map :

$$M : X \rightarrow g(X) \quad (34)$$

be equal to $I = [\alpha, \beta]$, where α and β ($\alpha < \beta$) can be determined from (31)-(33). In order to simplify the calculations, let us change the variable X into X' so that the interval I is transformed into $[0, 1]$. This corresponds to the change of variable :

$$X = (\beta - \alpha)X' + \alpha \quad (35)$$

then, the map

$$M' : X' \rightarrow g'(X') = \frac{1}{\alpha - \beta} g \left(\frac{1}{\alpha - \beta} (X' - \alpha) \right) - \alpha \quad (36)$$

has an invariant interval $[0, 1]$. The graphs of the functions $g(X)$ and $g'(X')$ are similar : the first one can be obtained by multiplying the second one by $(\beta - \alpha)$ and by translating it by α . The slopes are obviously conserved by such a transformation.

3.3.2 Stability windows for the piecewise linear map M'

In this part we shall study the dynamics of the map M' defined in (36), assuming that :

$$|m_0| \leq \frac{|E|}{\sqrt{2}} < 1 - R|m_0| \quad (37)$$

In this case, the map M' has two linear sections as shown in Fig.9b and can be represented as follows :

$$f : X \rightarrow \begin{cases} l_0 X + a, & \text{if } X \in [0, b] \\ l_1 X - l_1, & \text{if } X \in [b, 1] \end{cases} \quad (38)$$

where l_0 and l_1 denote the slopes of the left and the right segments, respectively, and where the parameters a and b are given by :

$$\begin{cases} a = 1 - l_0 \left(1 + \frac{1}{l_1} \right) \\ b = 1 + \frac{1}{l_1} \end{cases} \quad (39)$$

The map M' has one break point at $X = b$, where $M(X)$ is equal to 1. The slope is equal to l_0 in the interval $[0, b)$ and to l_1 in $(b, 1]$. As it has been shown in the study of the time-delayed circuit, the map must be studied in the region of the (l_0, l_1) -plane:

$$\pi : \begin{cases} 0 \leq l_0 \leq 1 \\ -\infty < l_1 \leq -1 \end{cases} \quad (40)$$

The two inequalities (40) are equivalent to: $0 < 1 - b \leq a \leq 1$

Note that the slope l_0 and l_1 can be obtained directly from the parameters of the time-delayed Chua's circuit:

$$\begin{cases} l_0 = \frac{-Z + (Z - R)m_0}{Z + (Z + R)m_0} \\ l_1 = \frac{-Z + (Z - R)m_2}{Z + (Z + R)m_2} \end{cases} \quad (41)$$

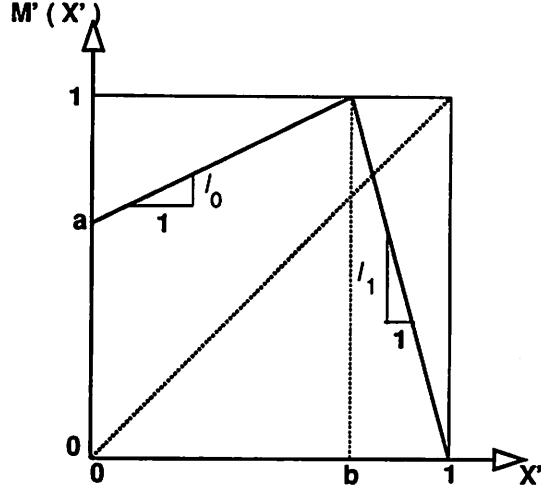


Figure 10: Map M'

(see formulas (28)).

Stable cycle of period 2 The inequalities (40) imply the existence of a single cycle of period 2:

$$\left(X_0 = \frac{l_0(l_1+1)}{l_0 l_1} \quad , \quad X_1 = \frac{l_0 l_1 (l_1+1) l_0 - 1}{l_1 (l_0 l_1 - 1)} \right) \quad (42)$$

The stability condition of this cycle is $l_0 l_1 \geq -1$. Therefore the condition for the existence *and* stability of a limit cycle of period 2 is :

$$\begin{cases} -\frac{1}{l_0} \leq l_1 \leq -1 \\ 0 \leq l_0 \leq 1 \end{cases} \quad (43)$$

Stable cycle of period 3 The map M' has a period-3 cycle if the first iteration of the point $X = 0$ is less than b , i.e. $a \leq b$. In terms of the parameters l_0 and l_1 , this is equivalent to $l_1 \leq -1 - \frac{1}{l_0}$. In this case the condition for the stability is $l_0^2 l_1 \geq -1$. Therefore the condition of existence *and* stability of a limit cycle of period 3 is :

$$\begin{cases} -\frac{1}{l_0^2} \leq l_1 \leq -1 - \frac{1}{l_0} \\ 0 \leq l_0 \leq \frac{-1+\sqrt{5}}{2} \end{cases} \quad (44)$$

Stable cycle of period n The condition for the existence of a limit cycle of period n: $\{X_1, X_2, \dots, X_n\}$, where :

$$\begin{cases} X_i < X_{i+1} \\ f(X_i) = X_{i+1}, \text{ for } i = 1, \dots, n-1 \\ f(X_n) = X_1 \end{cases} \quad (45)$$

is that the $(n - 2)$ th iteration of the point $X = 0$ is less than b , i.e.

$$l_0(\dots l_0(l_0 a + a) + a + \dots) + a < b \quad (46)$$

which can also be expressed by the inequality:

$$l_1 \leq -1 - \frac{1}{l_0} - \dots - \frac{1}{l_0^{n-2}} \quad (47)$$

The condition for the stability of this period- n cycle is : $l_0^{n-1} l_1 \geq -1$. Therefore the condition for the existence *and* stability of a limit cycle of period n is :

$$-\frac{1}{l_0^{n-1}} \leq l_1 \leq -1 - \frac{1}{l_0} - \dots - \frac{1}{l_0^{n-2}} \quad (48)$$

The curves $l_1 = -1 - \frac{1}{l_0} - \dots - \frac{1}{l_0^{n-2}}$ and $l_1 = -\frac{1}{l_0^{n-1}}$ are both monotone increasing and have one intersection point $O_n = (l_{0,n}, l_{1,n})$ in the region π defined in (40). The value of $l = l_{0,n}$ is determined as a solution of the algebraic equation:

$$l^{n-1} + l^{n-2} + \dots + l = 1 \quad (49)$$

which is equivalent to $l^n - 2l + 1 = 0$ and has one root in $[\frac{1}{2}, 1]$. $\{l_{0,n}\}_2^\infty$ is monotone decreasing and has a limit equal to $\frac{1}{2}$. Assuming that $l_{1,n} = -\frac{1}{l_{0,n}^{n-1}}$ (see (48)), it is obvious that $\{l_{1,n}\}_2^\infty$ is also monotone decreasing and tends towards $-\infty$. The points $O_n, n = 1, 2, \dots$ lie on the hyperbola:

$$l_1 = -\frac{1}{2} - \frac{1}{2(2l_0 - 1)} \quad (50)$$

The regions of the existence and stability of cycles of period 1,2,3,4 and 5 are shown in Fig.11 where the following notations are used :

$$\left\{ \begin{array}{l} (A, n) \quad - \quad \text{curve of emergence of a period-}n \text{ cycle} \\ (S, n) \quad - \quad \text{curve of loss of stability for a period-}n \text{ cycle} \\ \pi_n \quad \quad - \quad \text{region of existence and stability of a period-}n \text{ limit cycle} \end{array} \right.$$

Observe from Fig. 11 that chaos occurs in the area between every two consecutive stable regions. Moreover, since limit cycles of all periods occur consecutively, the time delayed Chua's circuit exhibits the *period-adding* phenomenon ⁴, which has so far been observed only in *non-autonomous* electronic circuits.

3.3.3 Histograms

As we shall see, the histogram gives us valuable informations on the dynamics of the map M . It gives the probability that M^n has a certain value within the invariant interval, for n large. In order to build this histogram, let us first divide the invariant interval I into N equal sub-intervals $I_{i \in [0..N-1]}$. Schematically, a histogram could be generated as follows: We choose an initial point X_0 in I , we calculate $M^n(X_0)$ for $n \in [0, K]$ where K is a large integer and we count how many times $M^n(X_0)$ visits each interval I_i . This can easily be interpreted as the history of the dynamics. However, if we consider only one initial point X_0 , it might for example belong to a limit cycle and we might miss the rest of the dynamics. Therefore we shall iterate this process starting from the N points x_i , defined as the midpoint of the sub-intervals I_i . In order to give a rigorous definition of the histogram, let us now define the functions h_i for $i \in [0, N - 1]$ as follows :

$$\begin{cases} h_i : R \rightarrow \{0, 1\} \\ x \rightarrow 1 & \text{if } x \in I_i \\ x \rightarrow 0 & \text{if } x \notin I_i \end{cases} \quad (51)$$

The histogram is the function H :

$$\begin{cases} H : \{0, 1 \dots N - 1\} \rightarrow \frac{N}{\sum_{j=0}^{N-1} \frac{\sum_{n=n_1}^{n_2} h_i(M^n(x_j))}{N(n_2 - n_1 + 1)}} \\ i \rightarrow \end{cases} \quad (52)$$

where n_1 and n_2 are two integers with $n_1 < n_2$. n_1 is the value of n for which we start considering the values of M^n . n_1 iterations are omitted from the sum while the transient settles. The next $n_2 - n_1$ iterations are taken into account. Of course, the larger n_2 is, the more accurate the value of H will be. One advantage of this histogram is its rapid calculation; in practice $n_1 = 50$ and $n_2 = 500$ give good results. The smaller n_1 and n_2 are, the larger N can be chosen for the same CPU time, leading to smaller intervals I_i and therefore better precision.

Examples of histograms related to our study of periodic windows are given in Figs.12a-12l. In Figs.12a-12k, l_1 is fixed at $l_1 = -18$ and l_0 varies from $l_0 = 0.04$ to $l_0 = 0.49$. In Fig.12-a and 12-b, one can recognize a stable limit cycle of period 2 and 3, respectively. However in these two cases, the situation is different. In the first one all the points, except the fixed point, belong to the basin of attraction of the period-two limit cycle, but in the second case there is an uncountable set of chaotic points which does not belong to the basin of attraction of the period-three limit cycle. The Lebesgue measure of this set is zero and therefore it cannot be detected in the histogram.

Except for zero-measure sets, histograms constitute a robust and useful tool to understand the dynamics of a system. Their evolution is also essential for studying bifurcation phenomena. An example is given in Figs.12c-12g where one can find histograms corresponding to a bifurcation from a period-3 to a period-4 cycle. During these bifurcation phenomena, the system remains chaotic. At $l_0 = .28$, we reach the period-4 cycle. If we go beyond $(S, 4)$, at $l_0 = 0.48$, the histogram suggests the existence of chaotic oscillations between five intervals. Eventually, we are able to find in the map (38) cycles of arbitrarily high period. As an example, in Fig. 12-l, we give a period-10 cycle obtained for $l_0 = 0.4787$ and $l_1 = -720$.

4 Conclusion

Starting from an infinite-dimensional extension of Chua's circuit where $C_1 = 0$, we have first reduced the dynamics of the system to that of a two or three-segment continuous 1-D map. In the case of a 2-segment map (i.e. $|m_0| \leq \frac{|E|}{\sqrt{2}} \leq |1 - R|m_0|$), we have found analytically the equation of the boundaries of the stability regions of any period n . These regions are all non-empty. Since limit cycles of all periods occur consecutively, the *time-delayed Chua's circuit* exhibits the "period-adding" phenomenon, for the first time in an autonomous circuit.

Figure captions

- 1 Chua's circuit
- 2 Time-delayed Chua's circuit
- 3 v-i characteristic $i_R = G(v_R)$ of Chua's diode
- 4 Simplified time-delayed Chua's circuit at equilibrium
- 5 Characteristic of Chua's diode in the bases B, B_0, B_1 and B_2
- 6 Determination of the characteristic of Chua's diode by the four points P_1, P_2, P_3 and P_4
- 7 Single-valued and multivalued map M
- 8 Map in the case $R=0$ and $E=0$
- 9 Three-segment and two-segment map M in the case $R=0$ and $E \neq 0$
- 10 Map M'
- 11 Existence and stability regions of cycles of period 2,3,4 and 5
- 12 Examples of histogram for the two-segment map M'

References

- [1] M.P. Kennedy, "Robust OP Amp realization of Chua's circuit", *Frequenz*, vol. 46, no. 3-4, pp. 66-80, March-April, 1992.
- [2] A.N. Sharkovsky and E.Yu. Romanenko, "Ideal turbulence: attractor of deterministic systems", *Int. J. of Bifurcation and Chaos*, vol. 1, no. 1, pp. 31-36, March 1992.
- [3] J. Naguro and M. Shimora, "Self-Oscillation in a transmission line with a tunnel diode", *Proc. os the IRE*, August, 1961, pp. 1281-1291.
- [4] L.O. Chua, Y. Yao, and Q. Yang, "Devil's staircase route to chaos in a nonlinear circuit", *Int. J. of Circuit Theory and Applications* , vol. 14, pp. 117-146, 1986.

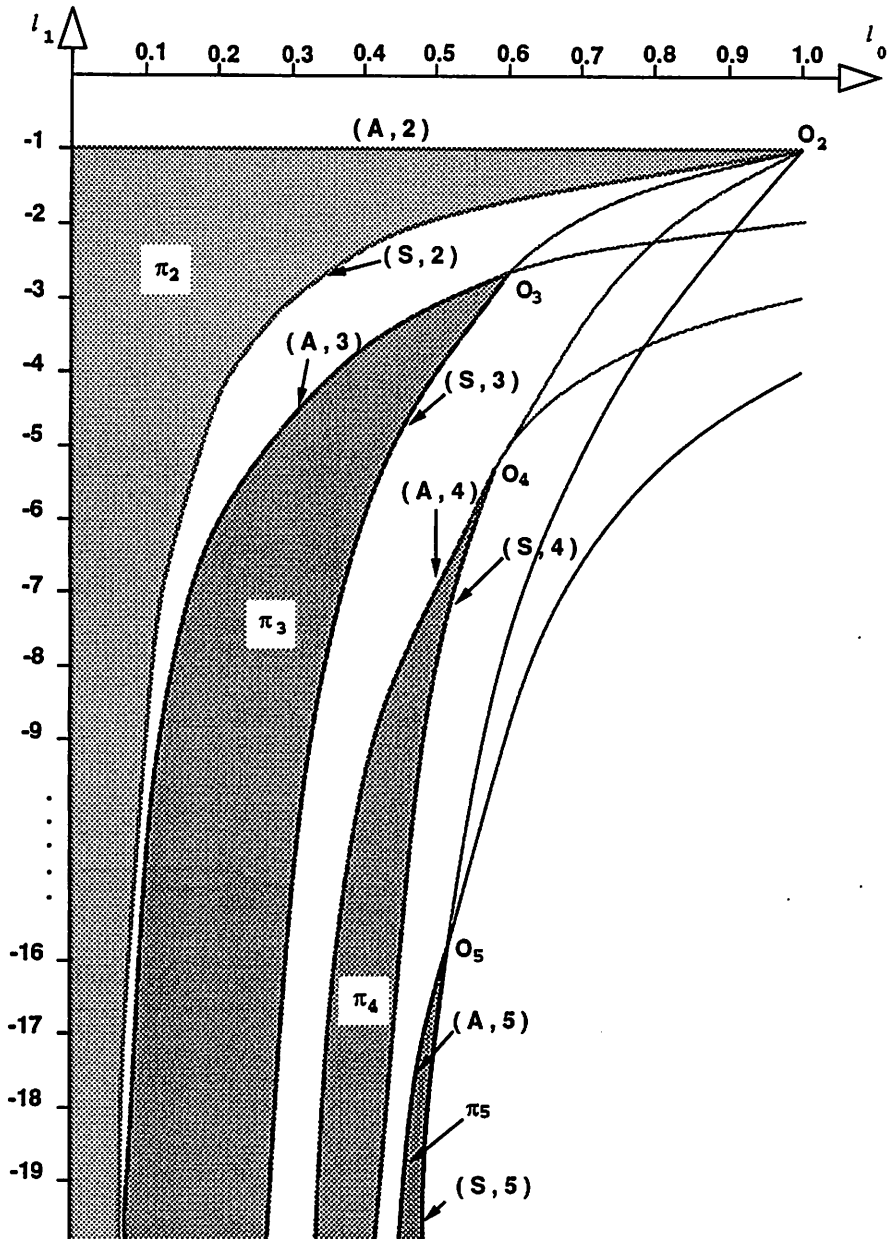
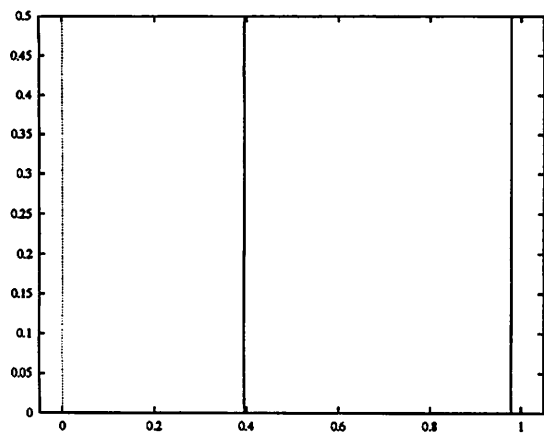
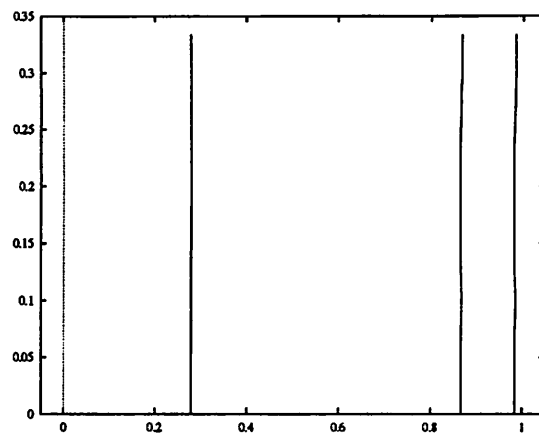


Figure 11: Existence and stability regions of cycles of period 2,3,4 and 5

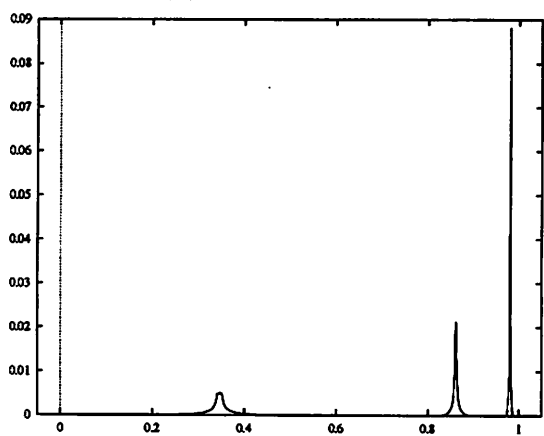
(a) $l_0 = 0.04$



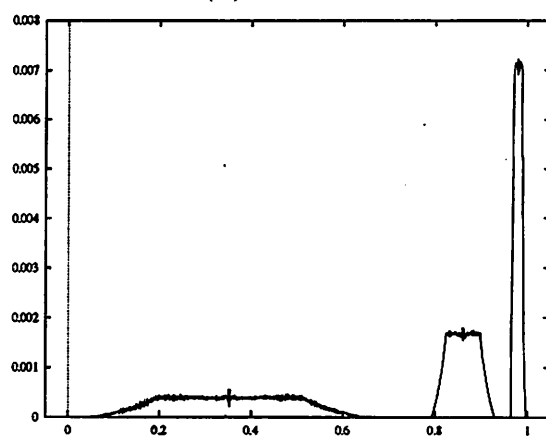
(b) $l_0 = 0.20$



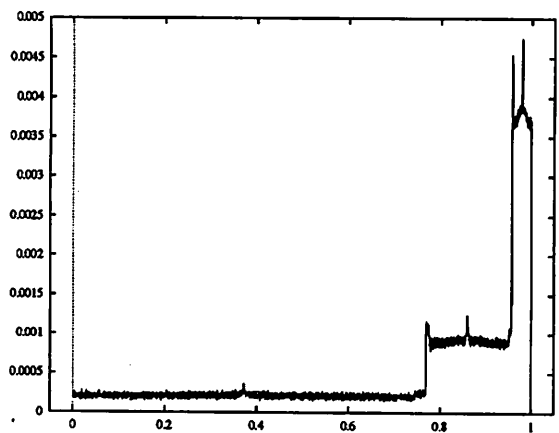
(c) $l_0 = 0.232$



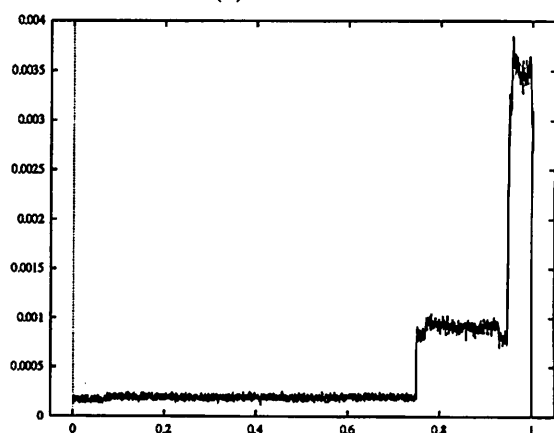
(d) $l_0 = 0.235$



(e) $l_0 = 0.245$



(f) $l_0 = 0.265$



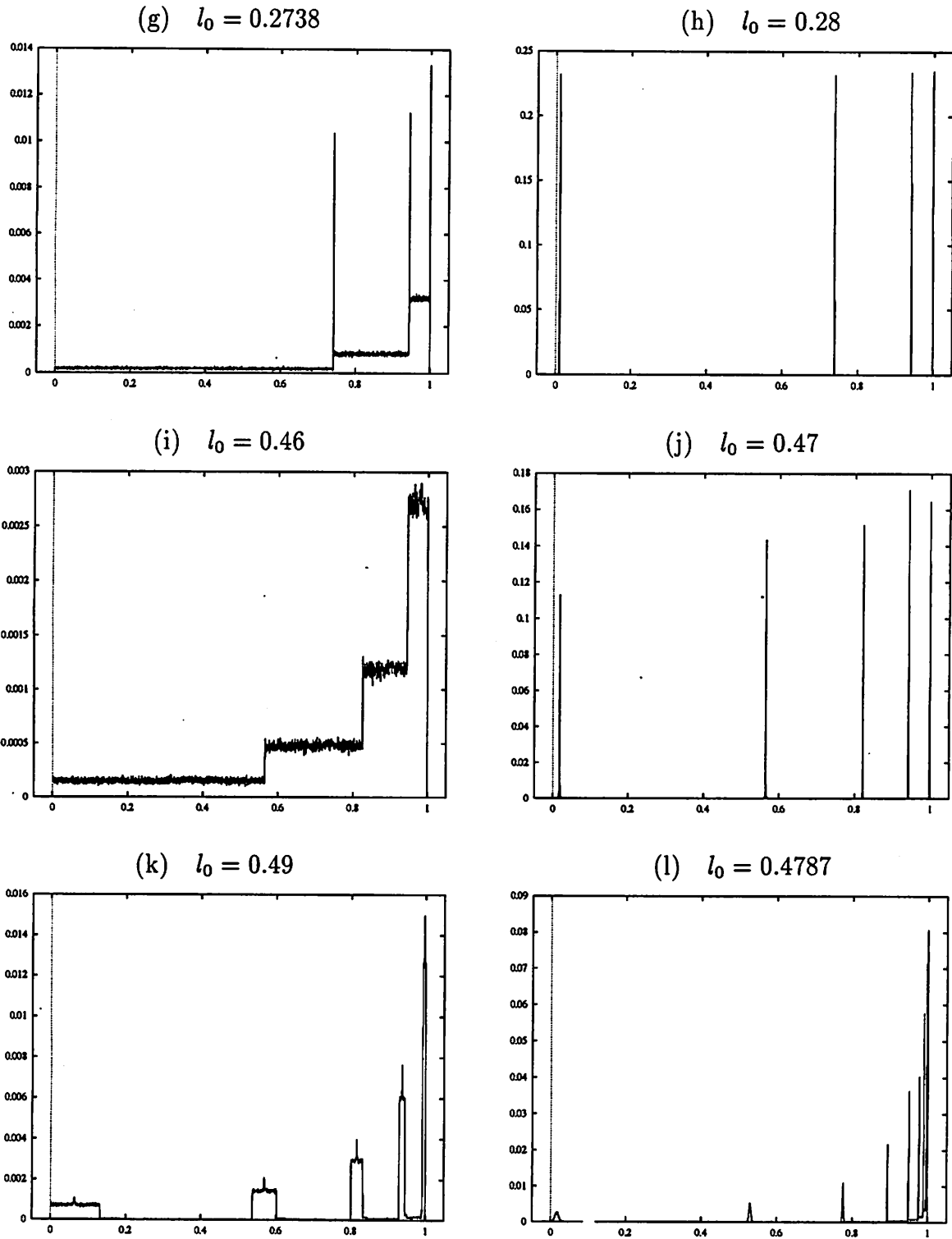


Figure 12: Examples of histogram for the two-segment map M'